Detecting the deformation of fast ice by InSAR technology with Sentinel-1A descending and ascending orbits data

LIU Jian[1,*], WANG Jinning[1], and WANG Zhiyong[1]

[1] College of Geomatics, Shandong University of Science and Technology, 266590, Qingdao, China; wjn2018sk@163.com (W.J.); wzywlp@163.com (W.Z.);

Abstract: Accurate mapping of fast ice deformation can effectively characterize the rheological behavior of fast ice and subsequently improve sea ice model. This study used the Sentinel-1A descending and ascending orbits data to detect the deformations of fast ice in the Baltic Sea. A method for automatically obtaining fast ice edge line by combining interferometric coherence image and SAR amplitude image was proposed. Then, the deformations of fast ice were detected from different incidence angles with the descending and ascending orbits data. The results showed that the deformations in radar line of sight obtained from the descending and ascending orbits data were 38cm and 37cm respectively within the fast ice region of 960km^2 in the study area. The continuous strong southwest wind was the principal reason for the deformation, and the deformation direction was dominated by east to west. Moreover, the inner fast ice kept stable and its deformation was smaller due to the protection of outer consolidated ice. The experimental results in this paper showed that the deformation trend and characteristics of fast ice can be better understood by InSAR technology with multi-orbits SAR data.

1 Introduction

Fast ice is a kind of stable sea ice that grows along the coast, islands, reefs andgrounding ice ridges and is firmly attached to them. During the ice season, people will create ice roads on thefast ice for the transport of large instruments and resources [1]. The thickness, area and stability of fast ice affect the safety of ships and ports.Its surface and interior may deform from several centimeters to tens of centimeters under the driving of external factors such as ocean current, strong wind and floating ice impact. When the stresses exceed the yield stresses, ice cracks will occur, which greatly threaten the personal safety. Therefore, it is very significant to detect the deformation, evaluate the possible destructive events, and make effective warning for local production and life in time and accurately.

InSAR (Synthetic Aperture Radar Interferometry) technology has been proved to be able to obtain micro-deformation in the detection of fast ice. InSAR technology has an important role and application prospect in studying the backscattering characteristics of fast ice which is（nearly）stationary and the small deformation of scattering sources[2].It can map fast ice with high accuracy and robustness in various environmental conditions by InSAR technology [3].Coherence images and interferograms are very significant for analyzing deformation features and estimating deformation factors.The precipitation and temperature rising could result in the decrease of coherence in fast ice, and the impacting of drift ice would cause a great impact on the fast ice boundary to produce dense fringes[4]. In addition, the fringe feature of interferogram can reflect the deformation trend of fast ice [5].According to the directions of interferometric fringes, the deformation can bedivided into different categories, and the potential dangers of the ice roads and the possibility of ice surface cracks can be warned[1].The deformations obtained by InSAR technology are in the radar line of sight (LOS). In order to better retrieve the deformation of fast ice, it is necessary to detect the deformation from different incident angles.

This paper took Bosnia Bay of the Baltic Sea as the research area and the deformations of fast ice were studied by InSAR technology with Sentinel-1A descending and ascending orbits data.Firstly, the boundary line of fast ice was obtained automatically by using the texture features of coherence image and SAR amplitude image. Then the deformations under different incidence angles were obtained by InSAR processing with descending and ascending orbits data. Finally, the deformation trend and factors were evaluated by comparing and analyzing the deformation characteristics.

2 Study region and data

The study area was the north part of the Bay of Bothnia in Baltic Sea (22.5°~25.5°E，65.0°~65.8°N), as shown in Fig. 1. The Baltic Sea is a semi-enclosed sea in the north

* Correspondence: LIU Jian, CYlovepeach@139.com; Tel.: +86 1573 263 1752

of Europe. Fast ice firstly grows along the coastline in the Bay of Bothnia in November each year, and it is rapidly expanded by attaching coastlines, islands, reefs and grounding ice ridges. The Baltic ice season generally lasts 5-7 months, from November of the previous year to May of the next year. The fast ice usually lasts throughout the ice season, especially in the Bay of Bothnia, where salinity is lower (less than 0.5 ‰ [4]). In order to avoid a series of disasters caused by sea ice, the monitoring of fast ice has always been the focus of attention in this area.

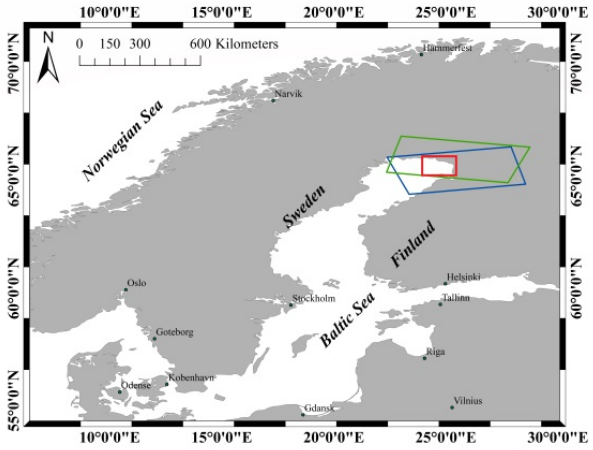

Fig. 1. Study area:The green and blue boxes represent the coverage of the images of descending and ascendingorbits respectively; the red box range represents the study region.

The study data were 4 SLC（Single Look Complex）with VV polarization products in IW (Interferometric Wide) mode of Sentine-1A. IW mode is featured by StripMap, which has three sub-swaths. The swath width is 250km, the spatial resolution is 5x20m, and the revisit period is 12 days.

Table 1. Characteristics of study data

Image pair	Acquisition date	Pass direction	Incidence angle
A	2018.02.02	Descending	41.06°
	2018.02.14	Descending	41.06°
B	2018.02.04	Ascending	36.12°
	2018.02.16	Ascending	36.12°

As shown in Table 1, Image pair A and image pair B were the interferometric pairs obtained by descending and ascending orbits data respectively,and the normal baselineswere 13.05m and 61.65m. The time baseline was 12 days, and the time difference between the two master images was 2 days. The same time baseline and similar imaging period ensured the consistency of experimental results. As auxiliary data, a lot of meteorological information was collected such as precipitation, temperature, wind speed, wind direction and sea level during the imaging period. These data were mainly from the meteorological observation station of Kemi Ajos (24.52°E, 65.67°N) [6].

3 Method

3.1 Observation difference between descending and ascending orbit

Fig. 2 was a schematic diagram of the deformation detection by descending and ascending orbit, in which θ_{inc}^{A} and θ_{inc}^{D} represent the incidence angles in ascending and descending orbit, respectively. If the surface deformations are dominated by the vertical direction, the deformations in LOS will be different in magnitude due to the different incidence angles, but the positive and negative signs (positive is uplift; negative is sink) are consistent. However, if the surface deformationsare dominated by the east-west direction, the deformationsin LOS with different incident angles are not only different in magnitude, but also in the opposite direction.

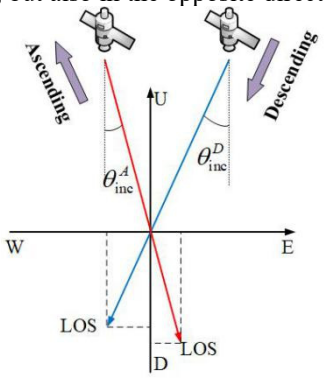

Fig. 2. A schematic diagram of the deformation detection: U-D and W-E represent up-down and west-east direction respectively.

3.2 InSAR processing

First, the baseline estimation was counted by using the master and slave images of the same orbit. Then, the master and slave images were co-registered at sub-pixel level using Sentinel-1A precise orbit data and external DEM data, and speckle noises were suppressed by multi-looking processing with the azimuth and range looks were 1 and 5 respectively. In order to further remove speckle noises, the Lee [7] algorithm with filtered window of 5×5 was used to filter SAR images. Next, the master and slave images after co-registered were conjugate multiplied to generate interferograms and coherence images. In order to optimize the phase unwrapping results and improve the visibility of the fringes, the flat phase was removed and the phase filtering was processed for the interferometric results. In this study, the flat phase was removed with the rough DEM, and the Goldstein algorithm was adopted for phase filtering [8]. After phase filtering, the minimum cost flow (MCF) algorithm was used to phase unwrapping [9]. Finally, the unwrapped phase was converted into displacement and geocoded, and the SAR image coordinate system was transferred to the mapping coordinate system.

3.3 Automatically extract fast ice boundary

First, SAR images should be segmented, and the data processing would be based on the segmentation units. As shown in Fig.3, the multi-resolution segmentation algorithm was used to segment the coherence images. Then, the threshold value was determined by Otsu algorithm [10] to obtain the sea ice region with high coherence value. Finally, several texture features were calculated by SAR amplitude images through GLCM operation, and the fast ice boundary was obtained by object-oriented feature extraction. A coastline data released by the GSSHG (Global Self-Consistent Hierarchical, High-resolution Geography database)of the NOAA (National Oceanic and Atmospheric Administration) was utilized as a land mask file for separating sea and land, and it also serves as the boundary line of the fast ice near the land side[11].

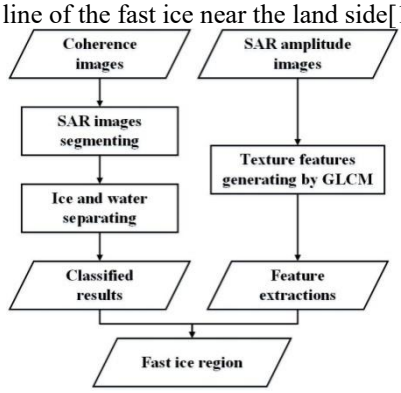

Fig. 3. Extracting fast ice boundary

4 Resultand analysis

The coherence images and interferograms were shown in Fig.4, in which the red and blue curves represent fast ice edge and coastline or islands, respectively.Fig.4a and Fig.4b were the coherence images obtained by image pair A and B, in which their mean coherence value were 0.5 and 0.47, respectively.Due to the shallow water that made the grounding of fast ice and the formation of ice ridges, the coherence values of the area near the shore decreased obviously. The values in the upper right corner of coherence images were also low because this area was the estuary of rivers, and the sea water was high fluidity and the warm river water raised the temperature of the sea area. Besides, the obvious changes of coherence image on the left of the fast ice edge line reflected that the sea ice in this area had changed greatly during the imaging period. Correspondingly, the interferometric fringes also changed greatly in the region where the coherence value changed.

On the one hand, the shape characteristics of interferometricfringes reflect the variation characteristics of ground surface deformations. The denser the fringesare, the more serious the deformations are. The change of each color cycle represents that the displacement change in LOS is about half wavelength length. The fast ice near the shore (right of fast ice boundary) had strong stability and small deformation, so the density of interferometric fringes was sparse, while the floating ice or consolidated ice (left of fast ice boundary) far away from the shore had poor stability and large deformation due to the influences of sea water, sea wind or impact of floating ice, so the interferometric fringes changed dramatically and the fringes were dense. On the other hand, the change of local regular fringes also reflected the change of deformation stress. For example, the interferometric fringes at the bottom of Fig.4dwere convex upward, which indicated that the sea ice in this area was likely to be subjected to the force from south to north.

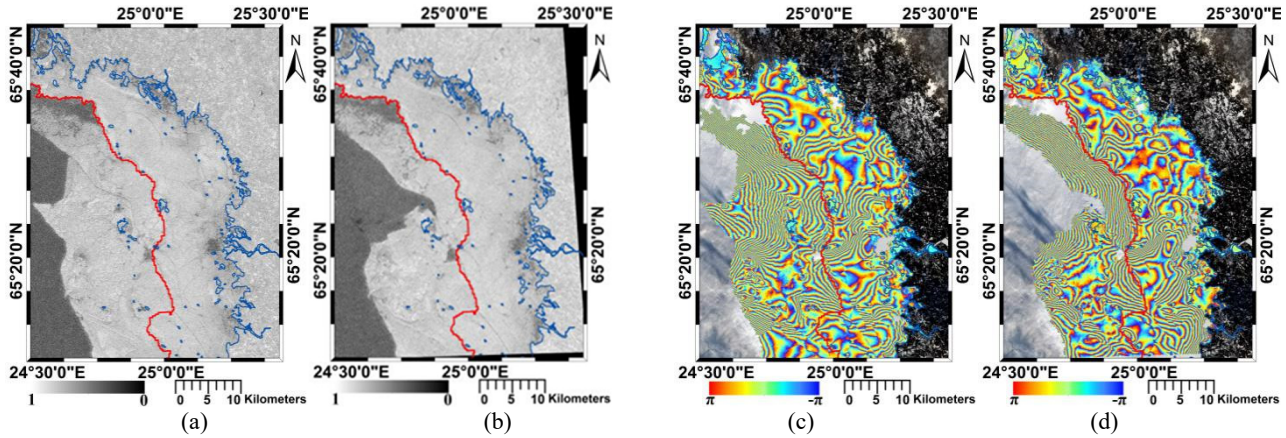

(a) (b) (c) (d)

Fig. 4. Coherence images and interferograms: (a) and (b) were coherence images obtained by image pair A and B, (c) and (d) were interferograms obtained by image pair A and B, respectively.

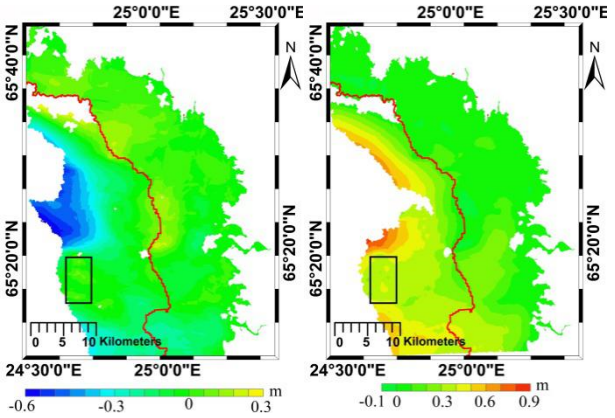

(a) (b)

Fig. 5. Deformation maps: (a) and (b) were deformation images obtained by image pair A and B.

The deformation map determined by image pair A was displayed in Fig. 5a, and the negative or positive sign represents the movement away from (sink or move to west) or close(uplift or move to east) to the satellite. Fig. 5b was the deformation result got by image pair B, but the same signs stood for oppositedeformation directions to that of Fig. 5a.

The results showed that the extreme displacement values occurred in the floating ice or consolidated ice, whilethe fast ice maintained a relatively stable state in the deformation results of both descending and ascending orbits, with small displacement variety. As shown in Table 2, the displacement values obtained from the descending and ascending orbits data were 38cm and 37cm, respectively.

Analyzing with auxiliary data, the continuous south and southeast winds existed during the image acquisition period with the speed over 12m/s. The winds caused the floating ice to drift towards the west, so the floating ice or consolidated ice took a larger displacement in Fig.5. The movements of floatingice also caused the impact and compression on the outer fast ice,which determined the characteristic of the interferometric fringes at the bottom of Fig.4d. As the protection of consolidatedice, however, the inner fast ice kept stable and its deformation was smaller. As refereed in Section 3.1, the same displacements in west-east direction will display in opposite sign in the deformation results that obtained by descending and ascending orbits data, sothe deformation directionwas mainly from east to west. Furthermore, the values in black rectangle in Fig.5 were both positive in descending and ascending deformation results,so the deformation might be dominated by uplift.

Table 2. Fast ice deformations

Directions	Deformation range/m	Displacement value/m
LOS（Descending）	-0.18~0.20	0.38
LOS（Ascending）	-0.07~0.30	0.37

5 Conclusions

In this paper, the deformation of fast ice in the Bay of Bothnia in Baltic Sea has been studied for a long time using InSAR technology with the descending and ascending orbits data of Sentinel-1A. A method for automatically obtaining fast ice edge line by combining interferometric coherence image and SAR amplitude image was proposed. During the study period, the results showed that the deformations obtained by the descending and ascending orbits datawere38cm and 37cm respectively within the fast ice region of 960km2 in the study area. The main reason for the rapid ice deformation was the shear stress caused by the drift of floating ice under the strong southwest wind, and the deformation direction might be mainly from east to west. In addition, the inner fast ice kept stable and its deformation was smaller due to the protection of consolidated ice. Compared with single orbit data, the deformations obtained by descending and ascending orbits data can better to analyze and understand the deformation trend and factors of fast ice. But, the InSAR deformation measurements are one-dimensional, i.e., in LOS. In further study,in order to accurately determine the nature of deformation, some multi-orbit data can be used to make the three-dimensional deformation of fast ice.

Acknowledgements

This study was supported by the National Natural Science Foundation of China (41876202) and the Natural Science Foundation of Shandong Province of China (ZR2017MD020).

References

1. D. O. Dammann, H. Eicken, et al. Cold Reg Sci Technol. Evaluating landfast sea ice stress and fracture in support of operations on sea ice using SAR interferometry.**149**, 51-64(2018)
2. P. B. G. Dammert , M. Lepparanta , J. Askne. Int J Remote Sens. SAR interferometry over Baltic Sea ice. **19**, 3019-3037(1998)
3. F. J. Meyer, A. R. Mahoney, et al. Remote Sens Environ, Mapping arctic landfast ice extent using L-band synthetic aperture radar interferometry. **115**, 3029-3043, (2011)
4. A. Berg, P. Dammert, L. E. B. Eriksson. IEEE. Trans. Geosci. Remote. X-Band Interferometric SAR Observations of Baltic Fast Ice. **53**,1248-1256 (2015)
5. M. Marbouti, J. Praks, et alal. Remote Sens. A Study of Landfast Ice with Sentinel-1 Repeat-Pass Interferometry over the Baltic Sea. **9**, 833(2017)
6. Ajos, Kemi Airport, Feb. 2018. [Online]. Available: https://www.timeanddate.com/weather/@661668/historic?month=2&year=2018
7. J. S. Lee. IEEE Trans. Systems, Man and Cybernetics. A Simple Speckle Smoothing Algorithm for Synthetic Aperture Radar Image. **13**, 86-89(1983)
8. R. M. Goldstein, C. L. Werner. Geophys. Res. Lett. Radar interferogram filtering for geophysical

applications. **25**, 4035 -4038(1998)

9. M. Costantini, IEEE Trans. Geosci. Remote Sens.A novel phase unwrapping method based on network programming. **36**, 813–821 (1998).
10. N. Otsu. IEEE Trans. Systems, Man and Cybernetics.A Threshold Selection Method from Gray-Level Histograms. **9**, 62-66(2007)
11. National Oceanic and Atmospheric Administratio n. [Online].Available: https://www.ngdc.noaa.gov/mgg/shorelines/data/gshhg/latest/